Robust multi-component modeling of diffusion tensor magnetic resonance imaging data

Yasser M. Kadah[*a], Xiangyang Ma[b], Stephen LaConte[b], Inas Yassine[a], and Xiaoping Hu[b]
[a]Biomedical Engineering Department, Cairo University, Giza, Egypt;
[b]Biomedical Engineering Department, Emory/Georgia Tech, Atlanta GA 30322, USA

ABSTRACT

In conventional diffusion tensor imaging (DTI) based on magnetic resonance data, each voxel is assumed to contain a single component having diffusion properties that can be fully represented by a single tensor. In spite of its apparent lack of generality, this assumption has been widely used in clinical and research purpose. This resulted in situations where correct interpretation of data was hampered by mixing of components and/or tractography Even though this assumption can be valid in some cases, the general case involves mixing of components resulting in significant deviation from the single tensor model. Hence, a strategy that allows the decomposition of data based on a mixture model has the potential of enhancing the diagnostic value of DTI. This work aims at developing a stable solution for the most general problem of multi-component modeling of diffusion tensor imaging data. This model does not include any assumptions about the nature or volume ratio of any of the components and utilizes a projection pursuit based strategy whereby a combination of exhaustive search and least-squares estimation is used to estimate 1D projections of the solution. Then, such solutions are combined to compute the multidimensional components in a fast and robust manner. The new method is demonstrated by both computer simulations and real diffusion-weighted data. The preliminary results indicate the success of the new method and its potential to enhance the interpretation of DTI data sets.

Keywords: Diffusion imaging, magnetic resonance imaging, projection pursuit regression.

1. INTRODUCTION

Among the unique features of magnetic resonance imaging (MRI) is its ability to characterize several microscopic phenomena in vivo and noninvasively[1]. An interesting example is the mapping of diffusion. In its most basic form, diffusion imaging attempts to characterize the manner by which the water molecules within a particular location move within a given amount of time. Using a simple pulse gradient spin echo (PGSE) imaging sequence, it is possible to obtain a change of the MR signal that is related to the diffusivity of water in a certain direction[2]. Given that such diffusivity parameters vary with the geometry of the internal/external cellular space, it has an important value in discriminating between different tissue types as well as identifying abnormal variations in pathological states.

In order to avoid non-unique variations in measuring diffusivity parameters with the positioning of the subject, a more general characterization of the diffusion process was introduced based on diffusion tensors. The basic techniques in diffusion tensor imaging attempt to characterize the 3-D diffusion phenomena in terms of a 3-D Gaussian probability distribution[3]. Therefore, such representation is sufficient in terms of a 3×3 symmetric tensor, or the so-called "cigar-shaped" diffusion tensor representation. This tensor is usually computed using a 3-D sampling of the b-space (the space of the diffusion experiment b-values[1]) of measurement in the diffusion-weighted experiment[4]. While requiring only six equations to completely determine the diffusion tensor, more measurements are usually obtained and a least-squares solution is calculated for the tensor. Recent studies revealed several deviations from this simplified scenario. Several authors reported a non-mono-exponential behavior for the diffusion-induced attenuation in brain tissue in water and NAA signals[3]. Their study was based on a 1-D diffusion experiment and the results were fitted to bi- or tri-exponential functions. They indicated that high b values reveal more complex behavior and therefore their fit depended on the value of b used in the measurement. Hsu *et al.*[5] proposed a two-compartment model for the diffusion in fibers of the myocardium. They reported two fast and slow components in their study while assuming a slow-exchange process

* E-mail: ymk@ieee.org

Medical Imaging 2005: Physiology, Function, and Structure from Medical Images, edited by Amir A. Amini, Armando Manduca, Proceedings of SPIE Vol. 5746 (SPIE, Bellingham, WA, 2005) · 1605-7422/05/$15 · doi: 10.1117/12.596155

between the two. Inglis *et al.*[6] reported bi-exponential diffusion tensor measurements. They hypothesized that these components may represent the intra- and extra-cellular components in tissues. Clark *et al.*[7] reported variations of the apparent diffusion coefficient with the value of diffusion time. Their hypothesis was that such variations are important indicators of restricted flow, which present a potentially large diagnostic value. In a later study by the same group, Clark *et al.*[8] reported results of a two-tensor model for diffusion in the human brain. They measured the parameters of a mixture model composed of two weighted tensors. Their results indicated the presence of fast and slow diffusion components, and that each can be modeled by a unique tensor. They indicated that the use of high b value was essential to reveal the slow component of diffusion. Tuch *et al.*[9] noted that the DTI measurements could only resolve the imaging situations where the white matter fibers are strongly aligned. They presented evidence from high angular resolution diffusion measurements to show that the diffusion process can be modeled as independent mixture of ideal diffusion processes. They presented results for the case of a mixture of two diffusion tensors. The methodology used to obtain the mixture parameters was based on minimizing an error function using gradient descent technique. Beaulieu[10] discussed the possible sources that would cause diffusion to be anisotropic including geometric, structural and pathological conditions. His study concluded that the presence of such processes as restricted diffusion in certain directions may be used to account for the measured anisotropy in DTI measurements. Frank[11] reported a method for identifying the anisotropy in high angular resolution diffusion-weighted (HARD) imaging data without computing the actual tensor. Another study by the same author[12] developed a methodology for characterizing HARD data by decomposition into spherical harmonics. This approach allowed several modes of diffusion to be decomposed into separate channels that are different from those for eddy current artifacts. He studied the case of two fibers under different conditions and proposed an extension of his method to characterize multiple fiber scenarios. Given the complexity of such situations and the limitations on the spherical harmonics definitions in terms of rotations only, this might not be practical in many cases. Basser and Jones[3] discussed the possibility of mixture modeling of diffusion. Even though they indicated that this would present a more complete representation of the process, they argued that there are too many issues that need to be resolved before such modeling can be performed in practice. In particular, their hypothetical discussion indicated that such modeling would require a large amount of data to enable the estimation of model parameters and involve the computation of too many parameters. They suggested also that several problems had to be addressed in such experiments that included optimization of diffusion gradient directions and model order selection. They concluded that this area had many aspects that were yet to be investigated.

Observing that the diffusion along nerve fibers tend to be significantly larger than in other directions (Basser *et al.*[13]), track fiber directions were computed from diffusion tensor data. The basic idea is to eigen-decompose the diffusion tensor and use the eigenvector corresponding to the largest eigenvalue as the most likely fiber direction in a given pixel. This simplistic representation of the problem is often unsuitable for real data where fiber direction heterogeneity is common. As a result, several studies indicated practical problems with this approach (cf. Mori and van Zijl[14]). In general, ambiguity arises in situations where the direction of the fiber cannot be determined. For example, in voxels where the estimated diffusion ellipsoid takes the form of a pancake shape rather than a cigar shape, the tracking algorithms terminate, resulting in undesired disconnections in the resulting fiber tracks. Poupon *et al.*[15] reported problems with the tracking results when crossing fibers are encountered. They proposed a methodology whereby some a priori knowledge about the fiber tracks are embedded in the fiber tracking procedure to regularize the calculated fiber directions. Similar regularization was proposed by Bammer *et al.*[16] where they used a continuous representation based on B-spline modeling.

After the diffusion tensor principal directions are determined, the problem of finding the fiber paths from the diffusion vector field (or the so called tractography problem) is a challenging one. Several techniques were proposed to do that based on line propagation or energy minimization implemented in different manners to try to overcome the limitations posed by noise, limited resolution and direction heterogeneity of fibers within the resolution cell (cf. Mori and van Zijl[14], Lori *et al.*[17]). The general limitations of the available techniques are the speed of axonal reconstruction, robustness in the presence of anisotropy in the diffusion tensor (e.g., the pancake shaped tensor case), as well as the difficulty of validating the outcome and the different constraints used in this processing. None of the available tracking methods provided a vision for how tracking should be done in case axonal intersections are resolved within resolution cells. By comparison to the conventional situations, this problem seems far more challenging since it involves adding another dimension to the original formulation representing axonal anisotropy.

The goal of this work is to derive the methodology and apparatus for multi-axon fiber tracking based on high angular resolution diffusion-weighted acquisitions. We utilize a multi-compartmental model to represent the physical make-up of imaging pixels. Based on an analytical expression of apparent diffusion tensor, the mixture model parameters are calculated using global nonlinear least squares methods. Given the characteristics of axonal membranes, the diffusion of water inside each axon is preferred along the direction of the axon than across it. Therefore, the diffusion from individual axons appears as a cigar-shape tensor. The presence of many fibers in the same direction results in an effective tensor that has the same shape as one of them. This simplified case is usually in fiber tracking. Here, we allow heterogeneity to be included in the analysis by proposing a pixel model with multiple tensors instead of one. Given the nonlinearity of the parameter estimation problem here, global nonlinear least-squares methods are utilized to compute the solution.

2. METHODS

2.1. Problem formulation

Consider the problem of estimating the composition of a voxel with two distinct components (without loss of generality for multiple components). In this case, the number of unknowns to fully describe the model is 13 (2 symmetric tensors and their partial volume ratios that sum to one). Unlike the problem of estimating a single tensor, the equations here are nonlinear and therefore only iterative techniques can be utilized. We observe that the attenuation equation for each tensor resembles a sample of a 3D Gaussian function with a covariance matrix equal to the diffusion tensor evaluated at a point determined by the diffusion gradient direction at a radius equal to the square root of the b-value. Hence, the problem of estimating multiple tensors becomes one of 3D Gaussian mixture modeling from samples determined by the diffusion gradient vector sampling.

To overcome this difficult estimation, we propose the use of projection pursuit regression (PPR), a robust statistical tool that allows the estimation of such mixture models[18-19]. Instead of attempting the solution in the high dimensional space of this problem, PPR projects the problem into a number of 1D problems and then synthesizes the solution to the original problem space. Moreover, the problem can be simplified further by utilizing a sampling strategy that converts the problem into the sum of two exponentials. This problem is solved using a robust strategy in which the exponential decay constants are estimated using exhaustive search and the magnitude functions are estimated using linear system solution based on the choice of the decay constants. Given that the range of decay constants for human applications is rather limited, this strategy has superior speed to nonlinear least squares methods while offering the global solution to the problem. Once the 1D model is estimated, it can be used to provide an equation for each diffusion tensor separately as identified by its partial volume ratio. For example, we identify the components with the larger partial volume ratio as component #1 in all projections and utilize such projections to reconstruct its tensor the same way the single-tensor method works. Then, the second tensor is computed based on projections with second largest partial volume ratio and so on for other components (if exist). The computed tensors are used to compute a new estimate of the component partial volume ratios based on the whole data set rather than each projection separately. Given that these ratios are the most affected by noise, the estimation process is started again with this new estimate plugged in for all projections and a new solution is estimated. This process is repeated until the partial volume ratio stabilizes. In the general case of a N-tensor model, the same procedure is followed at a computational cost that varies linearly with the number of tensors N. The following subsections detail the multi-tensor model estimation.

2.2. Estimation of 3D Gaussian function from its 1D projections

The NMR signal attenuation due to diffusion when applying a gradient defined by the direction $\vec{x}$ is given by,

$$E(\vec{x}) = \exp\left(-\pi \cdot \vec{x}^T \cdot D \cdot \vec{x}\right) \tag{1}$$

Here, *D* is the diffusion tensor and $\vec{x} \equiv \sqrt{b/\pi} \cdot \vec{u}$, with a unit vector $\vec{u}$ in the direction of the gradients at an applied b-value of *b*. In order to proceed with the projection pursuit strategy, we must to be able to relate the characteristics of the diffusion tensor D to the one-dimensional projection of this function at an arbitrary direction. In order to compute this projection, we start with a 3D Gaussian function perfectly aligned with the coordinate axes and apply the rotation transformation to obtain the general formulation of the problem. Then, we utilize the projection-slice theorem to simplify the derivation of the projection integral. We start with the simplest form of the diffusion attenuation defined as,

$$E(\vec{x}) = E([x \quad y \quad z]) = \exp\left(-\pi \cdot [x \quad y \quad z] \cdot \begin{bmatrix} \lambda_1 & 0 & 0 \\ 0 & \lambda_2 & 0 \\ 0 & 0 & \lambda_3 \end{bmatrix} \cdot \begin{bmatrix} x \\ y \\ z \end{bmatrix}\right) = \exp\left(-\pi \cdot \vec{x}^T \Lambda \vec{x}\right) \tag{2}$$

The Fourier transformation of this function is given by,

$$\Im\{E(\vec{x})\} = \exp\left(-\pi \cdot [f_x \quad f_y \quad f_z] \cdot \begin{bmatrix} 1/\lambda_1 & 0 & 0 \\ 0 & 1/\lambda_2 & 0 \\ 0 & 0 & 1/\lambda_3 \end{bmatrix} \cdot \begin{bmatrix} f_x \\ f_y \\ f_z \end{bmatrix}\right) = \exp\left(-\pi \cdot \vec{f}^T \Lambda^{-1} \vec{f}^T\right) \cdot \tag{3}$$

Here, we used the separability property to derive the 3D Gaussian Fourier transformation given the 1D transformation result. Consider now a diffusion tensor in a general direction given by,

$$D = R^T \Lambda R \ , \tag{4}$$

where *R* is an orthogonal transformation. Then, the Fourier transformation of this general case is given by,

$$\Im\{E(\vec{x})\} = \exp\left(-\pi \cdot \vec{f}^T R^T \Lambda^{-1} R \vec{f}^T\right). \tag{5}$$

From the projection-slice theorem, the projection along a particular direction corresponds to a slice in the Fourier domain. Suppose that we would like to obtain the projection along the line that makes angles (θ, ϕ, φ) with the coordinate axes respectively. We first notice that two angles are only sufficient to fully describe the required rotation given that the summation of the squares of the cosines of the three angles is equal to unity. To simplify the computation of the slice line (representing the Fourier transformation of the projection in the spatial domain), we apply a rotational transformation corresponding to the reverse of the line angle to align this line along the f_x axis. This rotation is computed as,

$$A(\theta, \phi) = \begin{bmatrix} \cos\theta & -\sin\theta & 0 \\ \sin\theta & \cos\theta & 0 \\ 0 & 0 & 1 \end{bmatrix} \cdot \begin{bmatrix} 1 & 0 & 0 \\ 0 & \cos\phi & -\sin\phi \\ 0 & \sin\phi & \cos\phi \end{bmatrix} = \begin{bmatrix} \cos\theta & -\sin\theta\cos\phi & \sin\theta\sin\phi \\ \sin\theta & \cos\theta\cos\phi & -\cos\theta\sin\phi \\ 0 & \sin\phi & \cos\phi \end{bmatrix}. \tag{6}$$

Hence, the line slice can be given as,

$$Slice = \exp\left(-\pi f_x^2 [\cos\theta \quad -\sin\theta\cos\phi \quad \sin\theta\cos\phi] D^{-1} \begin{bmatrix} \cos\theta \\ -\sin\theta\cos\phi \\ \sin\theta\cos\phi \end{bmatrix}\right) = \exp\left(-\pi \cdot f_x^2 \cdot \sigma^2\right). \tag{7}$$

Hence, the projection in the spatial domain can be given as,

$$projection = \exp\left(-\pi \cdot x^2 / \sigma^2\right). \tag{8}$$

Hence, if we measure the variance σ^2 of the projection function along at least six directions, we can directly compute the inverse of the diffusion tensor and subsequently the diffusion tensor.

2.3. Estimation of components from projections

Assuming a two-component model without loss of generality, the projection along any given direction can be given as,

$$p(x) = \alpha_1 \cdot \exp(-\pi x^2 / \sigma_1^{\ 2}) + \alpha_2 \cdot \exp(-\pi x^2 / \sigma_2^{\ 2}) \ . \tag{9}$$

Here, the relative amplitudes are given by α_1 and α_2 and the variances are generally different for both components and vary with projection direction. The x value is known and can be computed given the b-value and the direction of diffusion gradients. The 1D component estimation problem amounts to the estimation of α_1, α_2, σ_1 and σ_2 given $p(x)$. Notice that the component amplitudes are the same between projections. This property will be used to aid in the labeling of components among different projections. This estimation problem is nonlinear and therefore only iterative estimation methods have been proposed in the literature. Given the convergence issues associated with such methods and their generally high computational burden, another more stable strategy is needed to solve this problem in practice. Note that for any given parameter estimation accuracy, there exists a finite number of possible solution that are determined by the *a priori* information about parameter ranges and the desired accuracy. Hence, the problem of finding the solution to this

problem amounts to a combinatorial optimization problem. This means that a globally optimal solution can be found by exhaustive search or one of the more efficient random search strategies such as simulated annealing or genetic algorithms. Nevertheless, the computational effort involved in such techniques is prohibitive. Here, we combine exhaustive search and least squares estimation to obtain a more efficient implementation while maintaining the robustness and global optimality. In particular, instead of attempting to find all parameters by exhaustive search, we limit this strategy to those parameters of more importance in terms of accuracy and compute the remaining ones using least-squares estimation. This is implemented as follows:

Step 1. Take the variances to be the parameters estimated by exhaustive search while the partial volume ratios are estimated from them by least squares.

Step 2. Generate a list of possible values for the variances within the range from 0 to the maximum eigenvalue of the diffusion tensors of interest with the desired accuracy as the step.

Step 3. Plug in values for the variances in the equation from the list and compute the least-squares solution to the partial volume ratios for such values and compute the value of the residual error with such values plugged in.

Step 4. Loop on all possible variance values in the list and repeat step c and find the combination of values that generate the lowest error. Consider such combination to be the solution.

This method allows an order of magnitude saving in computation time while providing a solution with sufficient accuracy.

Once the individual component estimates from projections are computed, the projections of each component are used to estimate the component tensor in very much the same way as the single-tensor estimation is performed. One problem arises in this part because of component labeling. The basic assumption of the model that the partial volume ratios remain the same in projections may not be practical given the superimposed noise and other sources of error in DTI. In other words, partial volume ratios from different projections are different in practice. To solve this problem, an initial labeling is obtained whereby the first component is calculated from the projection components having the larger partial volume ratio, while the second component is calculated from the components with the smaller one. Once the two tensors are computed using this strategy, a least squares estimate for the partial volume ratios is computed while imposing the constraint of unit summation upon their values. Then, the calculated values are used in a second iteration of the procedure above to update the projection variances while imposing the same partial volume ratios obtained from the first iteration. A second estimate of the partial volume ratios is computed at the end of the second iteration and this process is repeated until estimates from two successive iterations differ by a predetermined tolerance. In this case, the estimates represent the global solution that is not biased by error within individual projections.

It should be noted that the extension of this method to multiple exponential is straightforward. The computational complexity of the developed method can be shown to depend linearly on the number of components. This allows the possibility of addressing more challenging tasks. We still gain the separation between the problems of estimating the variances and the magnitudes. Moreover, the same direct magnitude estimation method can still be applied in this case once the roots are calculated. This can, at least in principle, reduce the require complexity dramatically.

2.4. Projection direction selection

Continuing from the above to use the simpler multi-exponential model, the problem of determining the best directions for projecting the multi-component model will be addressed in very much the same way. Instead of seeking the directions representing the maximum non-Gaussianity as in the original formulation of the projection pursuit regression, we now see those directions representing the sharpest difference between the exponential decay constants. An excellent direction index for this purpose is the quantity under the square root in the second-degree characteristic polynomial root formula. Observing that this quantity is zero for equal roots and gets larger as the roots get apart, the maximization of this index provides a more efficient alternative to the kurtosis or other higher order moment optimization in the original Gaussian mixture model.

3. RESULTS AND DISCUSSION

To verify the new method, computer simulations were conducted to assess the accuracy of model estimation under different SNR and voxel tensor composition. The simulation parameters were as follows: the acquisition of one half of a cubic volume of size 8×8×8 voxels that fully covers the 3D extent of the diffusion attenuation. The data were projected

onto a number of directions that uniformly sample the space. For convenience, these directions were taken to be similar to those used in DTI acquisition as either 6, 12, 30 or 90 directions. Instead of selecting a few directions in the original PPR formulation, all directions are taken into consideration with a weighting corresponding to the model error. Also, within each 1D estimation procedure, a regularization step is implemented to verify that the partial volume ratio of all components is above a certain threshold value. This is necessary since it is likely that the component projections may have similar decay at some directions resulting in ill-conditioned solution. The simulation results of a model composed of both white matter (WM) and CSF are shown in Fig. 1. Notice that for SNR above 50 dB the estimation error of the tensors is below 10%. The model estimation procedure for each voxel was performed within an average of less than 1 sec (based on a 2 GHz P4 computer with 512MB RAM), which is reasonable for practical purposes.

Experimental results were also obtained from data sets collected from a normal human volunteer on a 3T Siemens Trio system using a double spin-echo sequence with 8 b-values spanning the range [0,1500] at 12 and 30 directions. Both scans were repeated 4 times to investigate the effect of SNR. The total scan time for the 12-direction scan was 12 minutes while it was approximately 30 minutes for the 30-direction scan. The iterative estimation procedure is illustrated for a single voxel in Figs. 2-3 where the fractional anisotropy[1] is computed for both components of the 2-tensor model to illustrate the convergence in both the 12- and 30-direction acquisitions. The estimation error for both cases is also shown in Fig. 3 where the convergence appears to occur within a few iterations. Table 1 shows the values of partial volume ratios obtained in such iteration, which also shows an important role for such iteration to significantly improve the accuracy of the results. The tensor field results from experimental data with 30 diffusion gradient directions and 4 averages are shown in Fig. 4 where the new method is compared to the 1-tensor model visually and using an error measure of the fitting accuracy. The tensors are drawn in such a way to show CSF tensors as points and white matter tensors as lines. As can be shown, the areas that show partial voluming at the interfaces of the CSF areas show significant improvement in model error when the 2-tensor model is used. A detailed view of another slice is shown in Figs. 5-6 where the tensor field is more visible. The average reduction in model error over the whole ROI was 30.1% for the 30-direction data set and 8.9% for the 12-direction data set (individual voxels exhibit error rates that are up to 80% lower in some cases).

With the encouraging results obtained, several applications should be addressed to verify the clinical utility of the new method. Examples include the removal of the effect of CSF contamination in both white matter and gray matter voxels, which cause significant problems in fiber tracking. Also, the ability of the new method to resolve crossing fibers needs to be verified with a controlled experiment where a known fiber crossing is present (e.g., a specially constructed phantom).

In spite of the visible improvement in residual error obtained with the new model, it is important to address several issues related to the regularization of the model to avoid erroneous interpretation of the results. For example, a threshold must be set for the partial volume ratio below which the component is discarded as nuisance. This can be done through a penalty term in the objective function that rewards lower order models. Also, given that the component characteristics in neurological applications are usually known *a priori*, it is advantageous to take such information into account in estimating the model whereby resulting tensors are penalized for their distance from the nearest component. This allows a clear segmentation of the data set as well which can be an important tool in subsequent fiber tracking.

4. CONCLUSIONS

A new fast and robust method to estimate a diffusion mixture model is presented. The main advantage of this approach is the elimination of dependence on a priori knowledge about the tensor composition, which allows more flexibility in practical applications. The new solution strategy offers a stable method to compute a multi-component model for diffusion tensor imaging data that is optimal in the least-squares sense. Preliminary results from computer simulations as well as experimental data acquired from normal human volunteers seem encouraging and suggest several uses of the new method is resolving partial volume problems of white matter/gray matter with cerebrospinal fluid as well as sensitivity to detect multiple white matter fibers.

Acknowledgements: This work was supported in part by the NIH (grants RO1MH55346, RO1EB00331, and RO1EB002009), the Georgia Research Alliance, and the Whitaker Foundation.

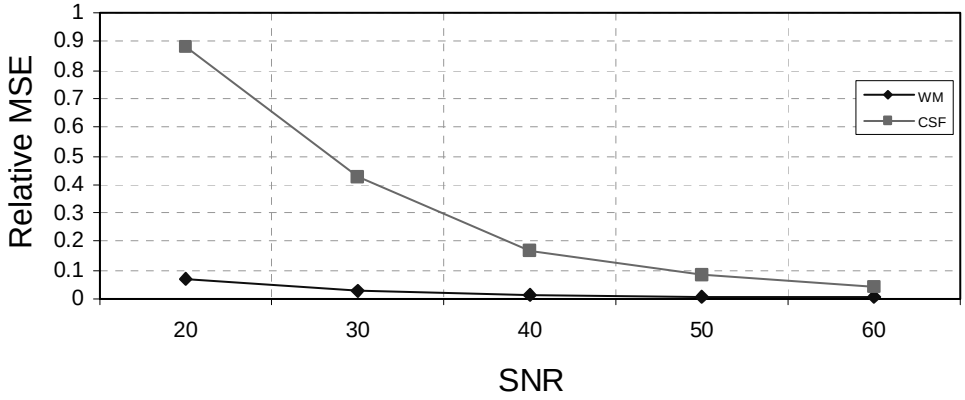

Figure 1: Monte Carlo simulations for the effect of noise on the multi-component model estimation

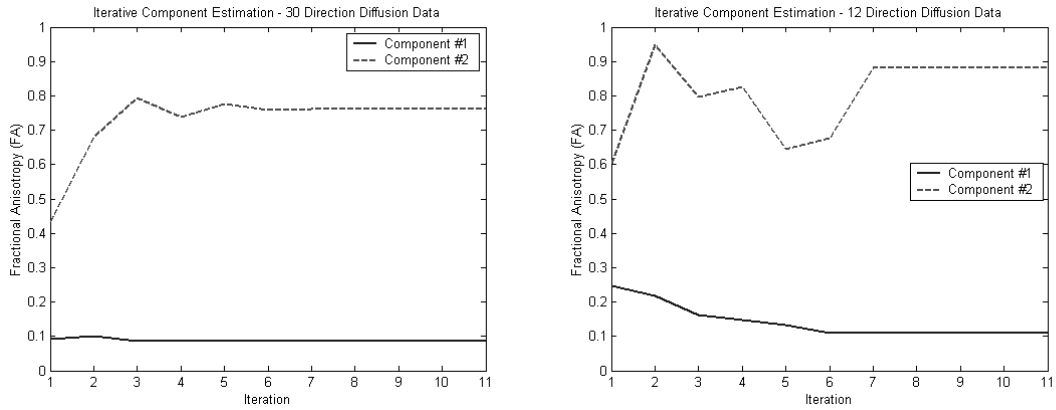

Figure (2): Illustration of the solution convergence in 2-tensor modeling as represented by the FA of components for both 12-direction and 30 direction data acquisition schemes.

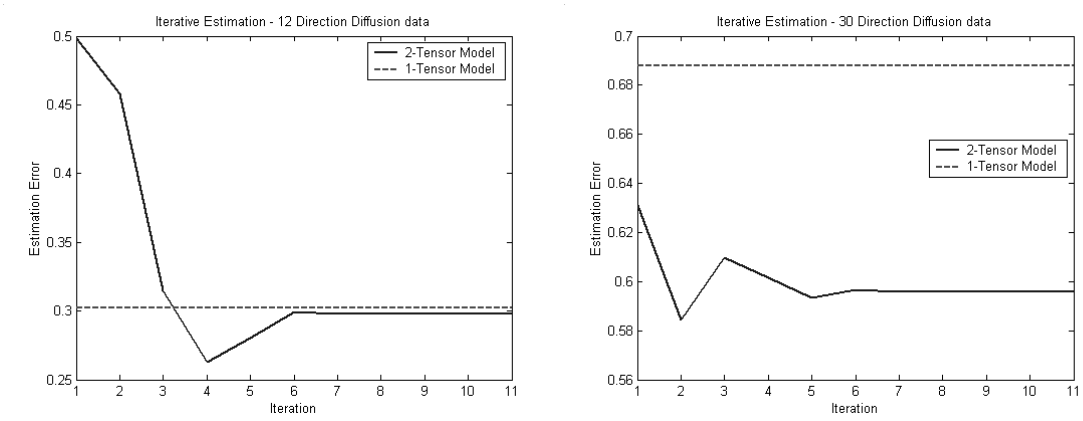

Figure (3): Illustration of the solution convergence in 2-tensor modeling as represented by the estimation error compared to 1-tensor modeling for both 12-direction and 30 direction data acquisition schemes.

Iteration	Partial Volume Ratio	**Model Estimation Error**
1	0.875628	3.06825
2	0.937119	1.74754
3	0.955467	0.918910
4	0.961860	0.709180
5	0.973721	0.627891
6	0.970746	0.535916
7	0.969907	0.556192
8	0.969907	0.556192

Table 1: Illustration of the iteration to find the correct partial volume ratio

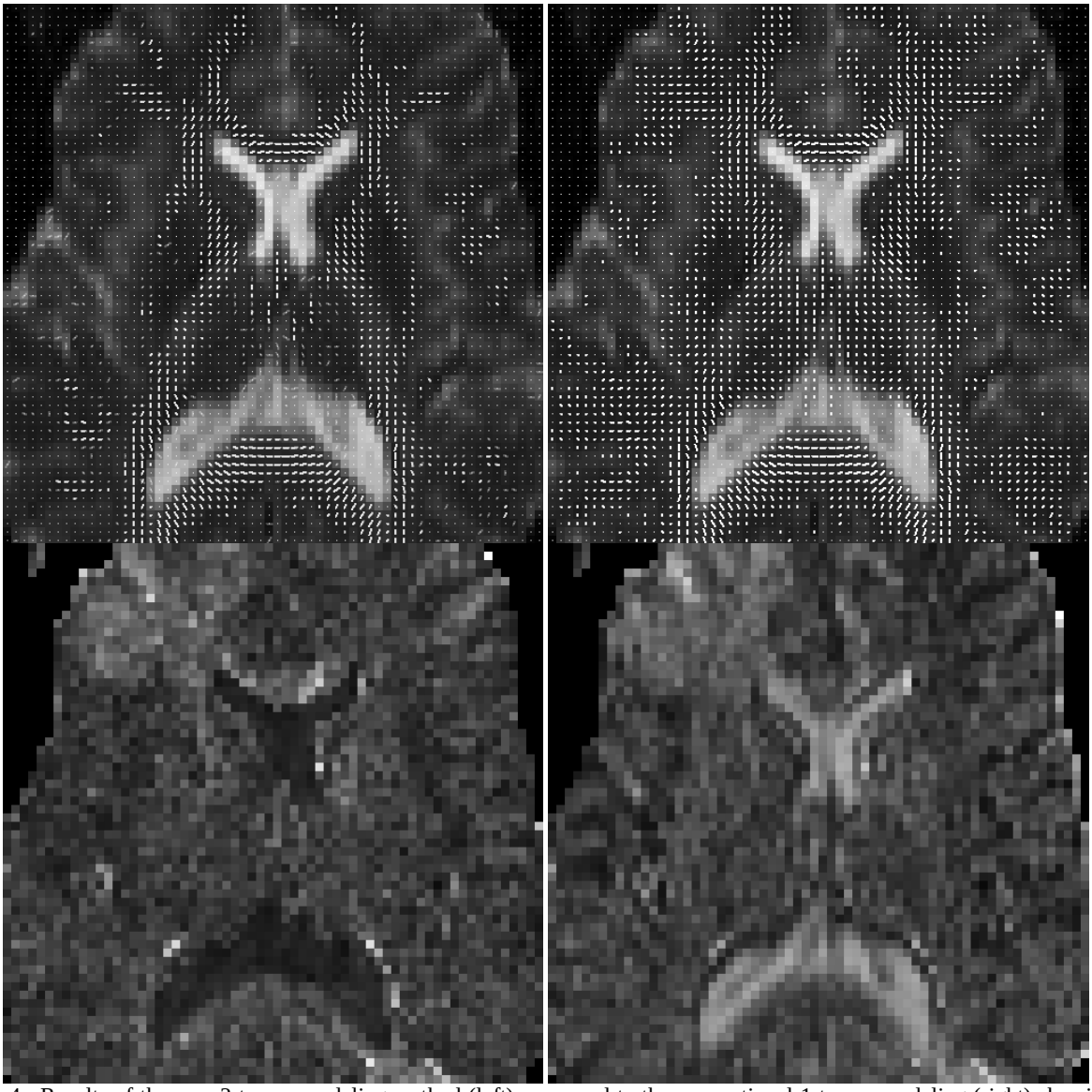

Figure 4: Results of the new 2-tensor modeling method (left) compared to the conventional 1-tensor modeling (right) showing the computed tensor field (top) and the residual error map (bottom). A significant reduction in errors is visible in regions where partial voluming is likely to occur such as near CSF.

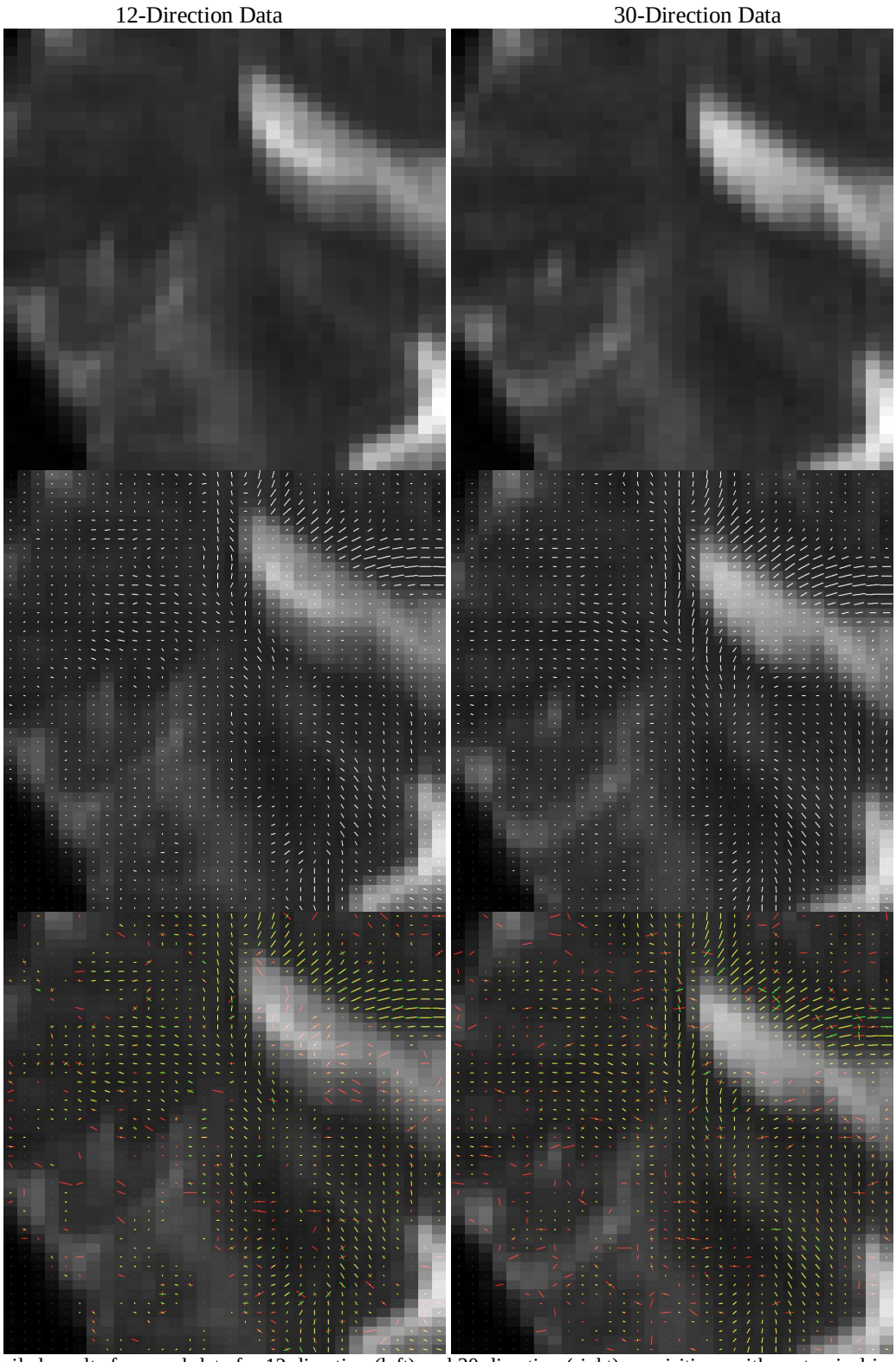

Fig. (5): Detailed results from real data for 12-direction (left) and 30-direction (right) acquisitions with anatomical images (top), 1-tensor model (middle) and 2-tensor model (bottom).

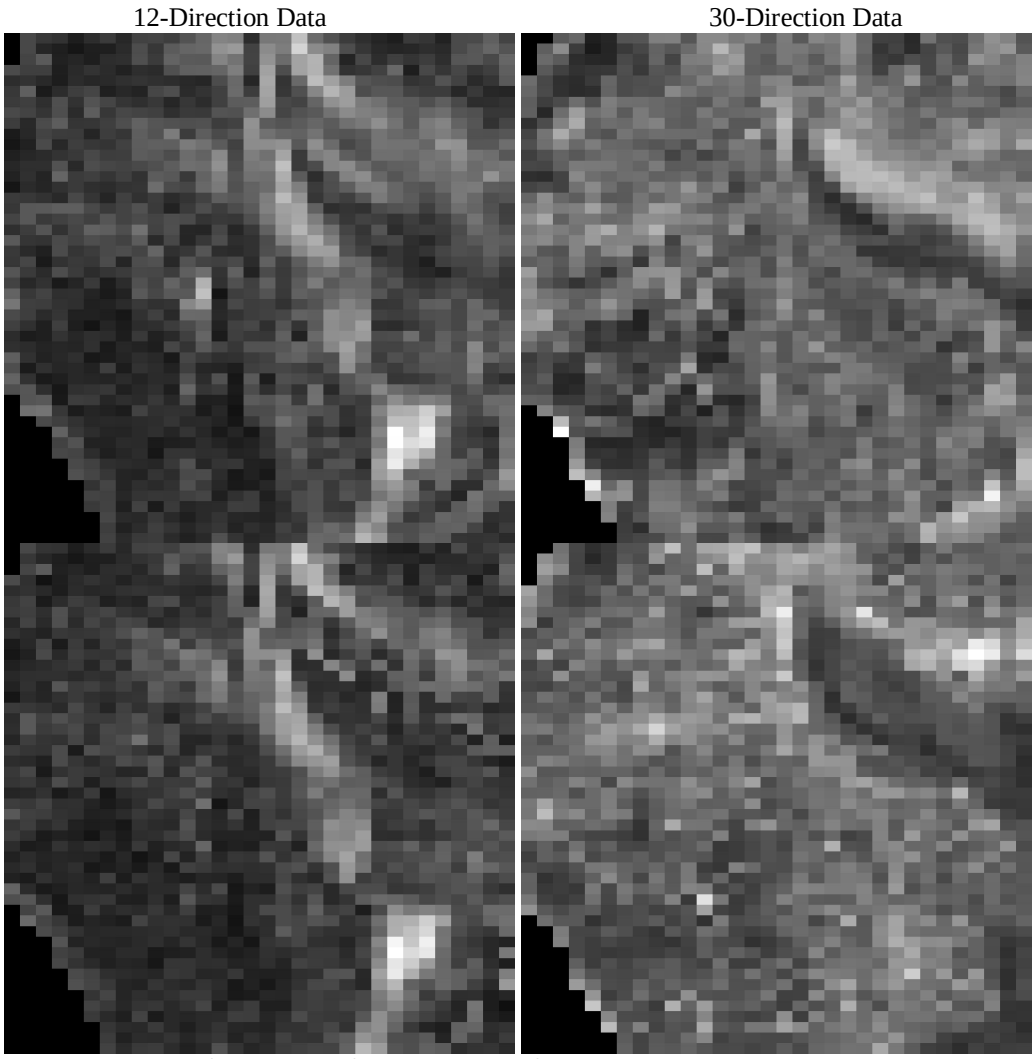

Figure (6): Estimation error maps from real data for 12-direction (left) and 30-direction (right) acquisitions with 1-tensor model error map (top) and 2-tensor model error map (bottom).

REFERENCES

1. D. Le Bihan, K.-F. Mangin, C. Poupon, C.A. Clark, S. Pappata, N. Molko, and H. Chabriat, "Diffusion tensor imaging: concepts and applications," *J. Magn. Reson. Imag*. **13**, pp. 534-546, 2001.
2. H.C. Torrey, "Bloch equations with diffusion terms," *Phys. Rev.*, vol. 104, no. 3, pp. 563-565, 1956.
3. P.J. Basser and D.K. Jones, "Diffusion-tensor MRI: theory, experimental design and data analysis – a technical review," *NMR Biomed*. **15**, pp. 456-467, 2002.
4. P.J. Basser, J. Mattiello, D. LeBihan, "Estimation of the effective self-diffusion tensor from the NMR spin echo. *J. Magn. Reson. B* **103**, pp. 247–254, 1994.
5. E.W. Hsu, D.L. Buckley, J.D. Bui, S.J. Blackband, and J.R. Forder, "Two-compartment diffusion tensor MRI of isolated perfused hearts," *Magn. Reson. Med.* **45**, pp. 1039:1045, 2001.
6. B.A. Inglis, E.L. Bossart, D.L. Buckley, E.D. Wirth III, and T.H. Mareci, "Visualization of neural tissue water compartments using biexponential diffusion tensor MRI," *Magn. Reson.. Med.* **45**, pp. 580-587, 2001.
7. C.A. Clark, M. Hedehus, and M.E. Moseley, "Diffusion time dependence of the apparent diffusion tensor in healthy human brain and white matter disease," *Magn. Reson. Med*. **45**, pp. 1126-1129, 2001.
8. C.A. Clark, M. Hedehus, and M.E. Moseley, "In vivo mapping of the fast and slow diffusion tensors in human brain," *Magn. Reson. Med.* **45**, pp. 623-628, 2002.
9. D.S. Tuch, T.G. Reese, M.R. Wiegell, N. Makris, J.W. Belliveau, and V.J. Wedeen, "High angular resolution diffusion imaging reveals intravoxel while matter fiber heterogeneity," *Magn. Reson. Med.* **48**, pp. 577-582, 2002.
10. C. Beaulieu, "The basis for anisotropic water diffusion in the nervous system – a technical review," *NMR Biomed.* **15**, pp. 435-455, 2002.
11. L.R. Frank, "Anisotropy in high angular resolution diffusion-weighted MRI," *Magn. Reson. Med.* **45**, pp. 935-939, 2002.
12. L.R. Frank, "Characterization of anisotropy in high angular resolution diffusion-weighted MRI," *Magn. Reson. Med.* **47**, pp. 1083-1099, 2002.
13. P.J. Basser, S. Pajevic, C. Pierpaoli, J. Duda, and A. Aldroubi, "In vivo fiber tractography using DT-MRI data," *Magn. Reson. Med.* **44**, pp. 625-632, 2000.
14. S. Mori and P.C.M. van Zijl, "Fiber tracking: principles and strategies – a technical review," *NMR Biomed*. **15**, pp. 468-480, 2002.
15. C. Poupon, C.A. Clark, V. Frouin, J. Regis, I. Bloch, D. Le Bihan, and J.-F. Mangin, "regularization of diffusion-based direction maps for the tracking of brain white matter fascicles," *Neuroimage* **12**, pp. 184-195, 2000.
16. R. Bammer, B. Acar, and M.E. Moseley, "In vivo tractography using diffusion imaging," *European J. Radiology* **00**, pp. 1-12, 2002.
17. N.F. Lori, E. Akbudak, J.S. Shimony, T.S. Cull, A.Z. Snyder, R.K. Guillory and T.E. Conturo, "Diffusion tensor fiber tracking of human brain connectivity: acquisition methods, reliability analysis and biological results," *NMR Biomed.* **15**, pp. 493-515, 2002.
18. J. H. Friedman and W. Stuetzle, "Projection pursuit regression," *J. Am. Stat. Assoc*. **76** (376), pp. 817-823, Dec. 1981.
19. J. H. Friedman, "Exploratory projection pursuit," *J. Am. Stat. Assoc.* **82** (397), pp. 249-266, Mar. 1987.